Effect of Kind and Content of Organo-Modified Clay on Properties of PET Nanocomposites

R. Scaffaro, L. Botta, M. Ceraulo, F. P. La Mantia

Dipartimento di Ingegneria Industriale, Università di Palermo, Viale delle Scienze, 90128 Palermo, Italy

Received 13 September 2010; accepted 4 January 2011
DOI 10.1002/app.34087
Published online 22 April 2011 in Wiley Online Library (wileyonlinelibrary.com).

ABSTRACT: In this work we report the properties of nanocomposite based on PET with two different samples of organically modified montmorillonites. In particular, we studied the effect of the filler concentration on morphology, rheology, and mechanical performance, focusing our attention on the effect of the degradation phenomena of the clay modifiers. The results indicate that at low clay level the morphology achieved is mainly intercalated. On increasing the filler level, coalescence and/or bad defragmentation phenomena induce a coarser morphology, as confirmed by XRD, SEM, and TEM observations. When a more polar organic modifier is used to modify the clay, the particle adhesion and distribution is slightly better. Conversely, at the processing temperatures adopted, this organic modifier induces a strong degradation of PET, as confirmed by melt rheology and intrinsic viscosity measurements. DSC indicates, in addition, a slight increase of crystallinity likely due to the decreased molecular weight. As regards the mechanical properties, Young's modulus is not significantly changed unless high amounts of clay (10%) are used while the elongation at break drops even at the lowest clay content. © 2011 Wiley Periodicals, Inc. J Appl Polym Sci 122: 384–392, 2011

Key words: nanocomposites; PET; organic modifier; degradation

INTRODUCTION

Poly(ethylene terephthalate) (PET) is a semicrystalline thermoplastic polyester widely used in textile fibers manufacturing, food packaging and liquid containers, thermoforming applications and engineering resins often in combination with fillers.

During the last years, there has been a growing interest to a class of polymer composites, called nanocomposites, based on the dispersion of fillers at a nanometric scale. Among the different kinds of nanoparticles, lamellar fillosilicates like montmorillonite and hectorite have been extensively studied.

Even if, except few cases, wide-scale applications of these materials are still not available, there is a large number of examples reporting improvements in the mechanical, barrier, and thermal properties.[1–8]

If the silicate tactoid completely delaminates, an exfoliated nanocomposite is obtained. Differently, if there is only an increase of the interlayer distance, the nanocomposite is called intercalated. Frequently, the morphology is a combination of the two above described. To improve and enhance the delamination and the adhesion with the polymeric matrix, clays are often modified with organic salts by cationic exchange reactions.

Among the possible different preparation methods, melt processing is more attractive than solution processing as it grants the possibility to obtain large amounts of material with a lower environmental impact due to the absence of solvent during processing. Actually, processes involving solvents can enhance the intercalation of the clays or, frequently, their complete exfoliation[9] but their scaling-up is so far very limited.

Among the different fillers, layered silicates were successfully used with polyesters.[10–20] In particular, organically modified clays were used to prepare PET-based nanocomposites via melt intercalation[13–16] or *in situ* interlayer polymerization.[17–20]

Aim of this work is to study the influence of different kinds of organically modified montmorillonites (OMM) on the rheological, mechanical, morphological and thermal properties of PET-based nanocomposites prepared by melt extrusion. In particular, the attention was focused on the effects of the degradation phenomena of PET and of the organic modifier of OMM on the nanocomposite properties.

Correspondence to: R. Scaffaro (roberto.scaffaro@unipa.it).
Contract grant sponsor: University of Palermo; contract grant number: ex 60% 2007.
Contract grant sponsor: MIUR; contract grant number: PRIN 2008.

TABLE I
Composition of Samples and Their Codes

Sample code	PET (wt %)	Cloisite 15A (wt %)	Cloisite 30B (wt %)
PET	100	–	–
PET/15A/3	97	3	–
PET/15A/5	95	5	–
PET/15A/10	90	10	–
PET/30B/3	97	–	3
PET/30B/5	95	–	5
PET/30B/10	90	–	10

EXPERIMENTAL

Materials and preparation

The polymer used in the frame of this work was a sample of bottle grade poly(ethylene terephthalate) (PET, Cleartuf P82, M and G Polimeri Italia S.p.A, Intrinsic viscosity = 0.82 dL/g, T_m = 249°C)).

Two commercial organoclays, supplied by Southern Clay Products, were used as nanofillers: Cloisite 15A (15A), a montmorillonite modified by 125 meq/100 g of dimethyl bis(hydrogenated tallow alkyl)ammonium cations and Cloisite 30B (30B), a montmorillonite modified by 90 meq/100g of bis(2-hydroxylethyl)-methyl tallow alkyl ammonium cations.

Both organoclays are commercialized under the form of white powder, with an initial average dimension of about 8 μm.

The nanocomposites were prepared by melt compounding using a Brabender counter rotating twin screw compounder (D = 45 mm; L/D = 7) with a thermal profile of 250–270–280°C at a rotational speed of 64 rpm. The polymer was processed with both the silicates at different concentrations: 3%, 5 and 10% by weight. In Table I there are reported the composition of all the samples and their identification codes.

For comparison, neat PET was processed under the same conditions adopted for the nanocomposites.

Samples for performing mechanical and rheological tests were prepared by compression molding using a Carver laboratory press (T = 285°C, P = 20 MPa).

To prevent hydrolytic degradation during processing, all the materials were dried in a oven vacuum for 24 h at 120°C prior to extruding them. The same treatment was performed on the extruded nanocomposite pellets before the preparation of the specimens for characterization.

Characterizations

The morphology of the prepared materials was evaluated by using scanning electron microscopy (SEM), transmission electron microscopy (TEM), and X-ray diffractometry (XRD).

Scanning electron micrographs (SEM) were obtained on samples fractured in liquid nitrogen and covered with gold to make them conductive, using a Philips ESEM XL30 scanning electron microscope.

Transmission electron microscopy (TEM) images were obtained with a JEM-2100 (JEOL, Japan) HR-TEM with 200 keV accelerating voltage. Ultrathin sections (80 nm thickness) of the specimens, cooled at −80°C, were obtained by cryoultramicrotomy with a diamond knife cooled at −60°C.

XRD analyses were performed using a diffractometer Siemens D-500 in reflection mode with an incident X-ray wavelength of 0.1542 nm.

Rheological measurements have been carried out by a parallel plate strain-controlled rheometer (Rheometrics RDA II, diameter of plates 25 mm) at 270°C. The instrument operated in the frequency sweep mode in the range 0.1–500 rad/s with a strain of 5%. The samples were dried under vacuum for 24 h at 120°C before testing.

Intrinsic viscosity measurements were performed at 30°C using an Ubbelohde viscometer. PET and all the nanocomposites were first dissolved in phenol/*o*-dichlorobenzene mixture (60/40 wt/wt) at a concentration of 0.2% wt/wt and at 50°C.

Intrinsic viscosity was calculated by using the Solomon-Ciuta equation:

$$[\eta] = \frac{\sqrt{2}}{c}\sqrt{\eta_{sp} - \ln \eta_{rel}} \quad (1)$$

where $[\eta]$ is the intrinsic viscosity, η_{sp} and η_{rel} the specific and the relative viscosity and c is the concentration of the polymer in solution.

A Perkin–Elmer DSC-7 was used for thermal analysis. The sample weight was around 12 mg for all the analyzed materials. The measurements were performed in the range 25–300°C, at a heating/cooling rate of 10°C/min.

Tensile mechanical properties were performed using a dinamometer Instron mod. 3365 on specimens (90 × 10 × ~ 0.6 mm) cut off from compression molded samples.

RESULTS AND DISCUSSION

X-ray diffractometry

To evaluate the morphology achieved by the OMMs in the polymer matrix, after processing operations, XRD diffraction has been carried out on all the prepared samples.

In Figure 1 there are reported the XRD patterns of the two organoclays and of the related nanocomposites.

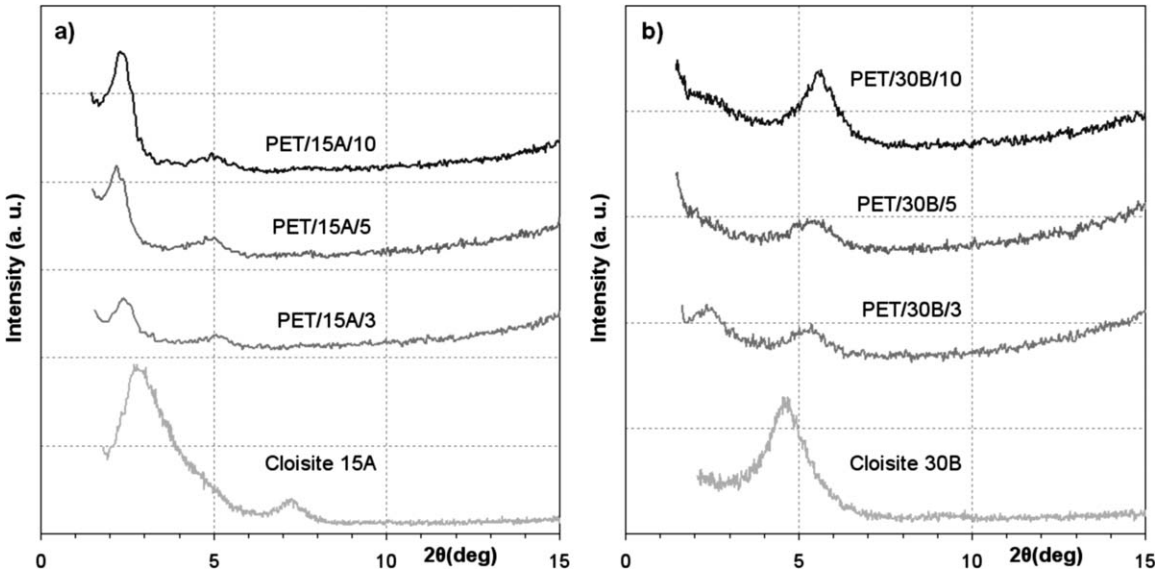

Figure 1 XRD patterns of the neat clays and of the nanocomposite materials: (a) Cloisite 15A and related nanocomposites; (b) Cloisite 30B and related nanocomposites.

In 15A XRD pattern, Figure 1(a), the peaks are broad and not in a harmonic series. This, according to the scientific literature,[21,22] can be explained considering a mixed structure of the silicate. In other words, there is the coexistence of different kinds of tactoids, not perfectly ordered or with different interlayer distances and this generates uncertainty in the univocal determination of the structure of the silicate. For 15A, this kind of structure can be reasonably explained with a different and nonuniform intercalation level of the organic modifier between the layers.[21]

The nanocomposites containing 3 and 5% of 15A show a shift of the peaks towards lower angles. In particular, the initial peak at 2.8° for neat 15A shifts to about 2.43° and 2.28°, respectively, for PET/15A/3 and PET/15A/5. These angles correspond to interlayer distances of 3.15 nm for neat 15A, 3.64 nm for PET/15A/3 and 3.87 nm for PET/15A/5 thus evidencing the formation of an intercalated structure. The situation is different when 10% of 15A is added. In this case, the peak at lower angles shifts to 2.35° with a corresponding interlayer distance to 3.77 nm. The decrease of the interlayer distance for this nanocomposite in comparison with PET/15A/5 is not surprising. The intercalation of polymer between the clay layers and the particles fragmentation is contrasted by aggregative forces. In other words, if the concentration is low enough, it is possible to achieve a steady expanded configuration of the clay tactoids but, if the concentration is relatively high, flocculation phenomena prevail and tactoids with a more compact structure are formed.[23]

30B XRD pattern, Figure 1(b), suggests similar considerations to those reported for 15A at least in terms of nonhomogeneity of the clay structure. Also in this case, in fact, there is no harmonic series of peaks and the most pronounced, at 4.67°, is extremely broad. Moreover, the global quantity of the organic modifier used in this clay sample is lower than that used for 15A and this may contribute to explain both the higher irregular structure and the sensibly lower initial interlayer distance.

This lack of homogeneity in the starting clay sample reflects in the nanocomposites. When 3% of 30B is added to PET two distinct broad peaks can be identified at lower and higher angles with respect to neat 30B. This can be likely due to the coexistence of two distinct kinds of structures. The peak at lower angles suggests the presence of an intercalated structure. This is expected based on the affinity of the organic modifier of 30B with the PET matrix: the related interlayer distance is 3.76 nm, even higher than that observed for the corresponding 15A containing blend. This is more relevant considering the initial interlayer distance of neat 30B, 1.89 nm, lower than that of 15A. Nevertheless, the peak at higher angles indicates a sort of collapse of the structure in some parts of the clay. On increasing the 30B level the situation is even worse. In this case, the peak at low angle disappears while the other gradually shifts toward higher angles, i.e., the clay presents smaller interlayer distances thus suggesting the collapse of the clay platelets.

The poor thermal stability of 30B[24–26] can be invoked to explain these results. At the top processing temperature adopted to prepare the nanocomposites

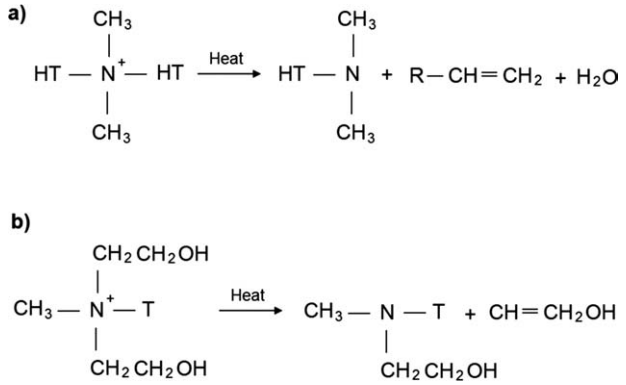

Figure 2 Schematic degradation paths of the organic modifier of : (a) 15A and (b) 30B.

(280°C) 30B showed a non negligible thermal instability that implies a progressive thermo-oxidative degradation of the organic modifier.

As reported by Shah and Paul[27] for other OMMs, it may be reasonably supposed that both the degradation and/or the volatilization of the organic modifier can cause its escape from the clay galleries that therefore progressively collapse, causing the shift of XRD peak to lower angle. Nevertheless, Gilman and coworkers[28] used XRD measurements to monitor the decrease of the interlayer spacing attributed to the collapse of the structure during the heating of nanocomposite, i.e., of the modified nanoclay.

It is worth nothing that both the OMMs, 15A and 30B, can undergo degradation phenomena during melt compounding. Indeed, as reported by other authors[26] the degradation starts at 182°C for 30 B and 208° for 15A.

As reported in the scientific literature,[16,24-27,29] the degradation of the organic modifier follows a Hoffman elimination mechanism that leads to the formation of α-olefins, amines and other products resulting from the secondary reactions between the degradation products within the organoclay as reported in the schematic degradation path in Figure 2(a) for the 15A. It was reported[16,24] that the organic modifier onto the montmorillonite surface may undergo thermal degradation inducing its elimination. In particular, the ammonium linkage on the clay is substituted by a hydrogen proton due to the β-carbon fracture. This latter, should act as Brønsted acid site, thus accelerating PET acidolysis.[16] Another acceleration of the degradation phenomena can be attributed to free water available in the system. Source of water are the dehydroxylation of the OMM during processing, Figure 2(a), and also the small fraction of adsorbed water present in the organoclays. Ultimately, the α-olefins, by-products, or intermediates produced in this reaction can attack the polymer and promote polymer degradation.

Paul and coworkers[25] suggested that, in the case of 30B, the activation of a hydroxyethyl group with an Al site of the organoclay may facilitate a Hoffmann-type elimination reaction as reported in the schematic degradation path in Figure 2(b) and, consequently, the polymer degradation. In addition the hydroxyl groups of 30B on the edges of the clay platelets can act as Brønsted acid sites thus accelerating PET degradation during the melt processing.[16]

Transmission electron microscopy

To better understand the structure of the nanocomposites and to corroborate the conclusions achieved by XRD analysis, TEM characterization was performed on the samples containing 3 and 10% of both clays.

The TEM micrograph of PET/15A/3, Figure 3a, clearly shows that the clay is organized in tactoids, suggesting that the structure of the nanocomposite is intercalated, thus corroborating the XRD analysis. In the PET/30B/3 system, Figure 3(b), the tactoids dimension decreases and isolated exfoliated structures can be found. This result can be explained considering the higher chemical affinity between 30B and PET in comparison with 15A that probably is not counterbalanced by the degradation phenomena that are less intense for the nanocomposite containing the lower content of 30B.

The TEM micrograph of PET/15A/10, reported in Figure 3(c), shows a tactoid formed by a greater number of clay sheets with a smaller interlayer distance in comparison with the nanocomposite containing only 3% of 15A. This result confirms the XRD analysis and in particular that a relatively high concentration of clay can provoke flocculation phenomena and the formation of tactoids with a more compact structure. This type of morphology is better evident for the PET/30B/10 system, Figure 3(d). Indeed, the micrograph shows a great collapsed tactoid formed by several clay sheets with a very small interlayer distance. Again, this result is in full agreement with the XRD measurements. As above commented, the reduction of interlayer spacing observed by XRD analyses and corroborated by TEM micrographs can be interpreted by considering that the organic modifier within the clay galleries decreased upon degradation thus causing the clay structure collapse[26,27]. In this case, probably the negative effect of degradation phenomena overcomes the positive effect of the higher affinity between 30B and PET.

Scanning electron microscopy

To evaluate the phase morphology of the nanocomposites and the dispersion of the filler, SEM analysis was performed. In Figure 4 there are reported the

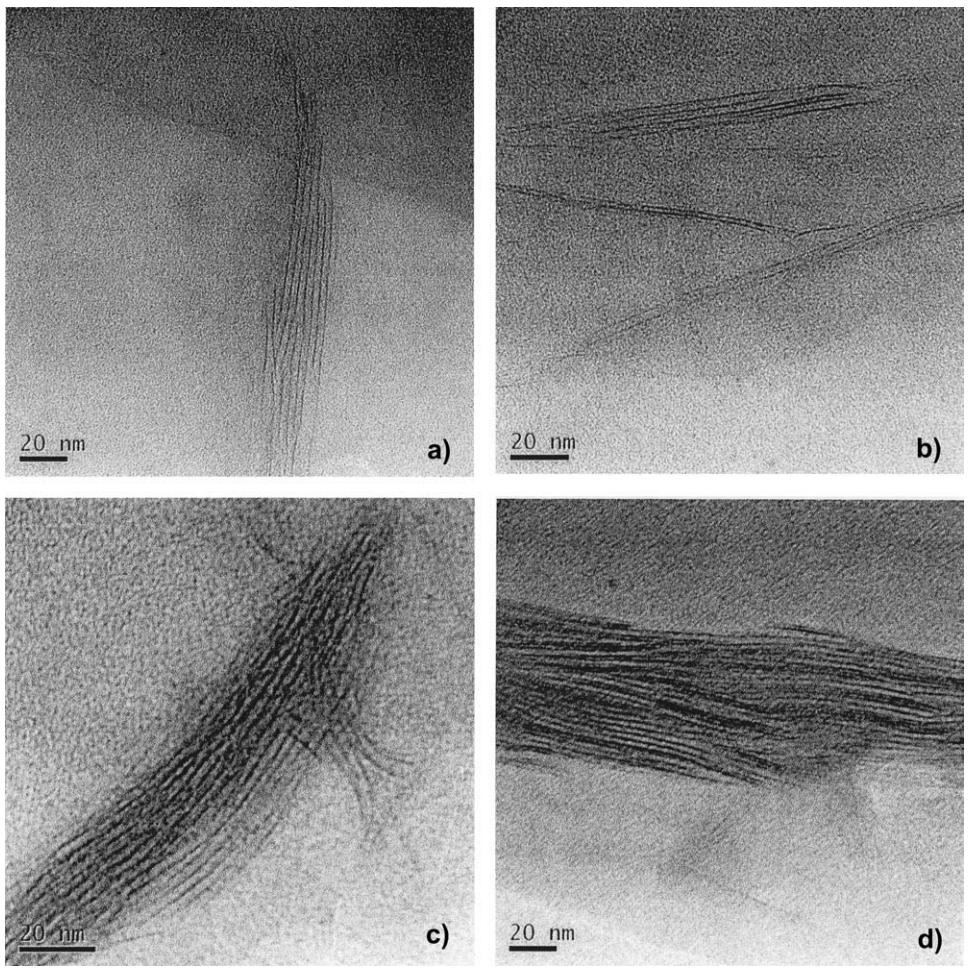

Figure 3 TEM micrographs of the nanocomposite materials: (a) PET/15A/3; (b) PET/30B/3; (c) PET/15A/10; (d) PET/30B/10.

SEM micrographs of the neat clays, Figure 4(a,e), and of all the nanocomposite materials prepared in the frame of the present work, Figure 4(b–d, f–h). In all the cases, it is evident that the dimensions of the clay particles are in the submicrometric scale, i.e., smaller than the initial ones, thus confirming that the melt extrusion caused a disaggregation of the clay clusters and the dispersion of the particles into the matrix.

It is worth noting that, for sake of clarity, the micrographs of neat Cloisite are reported at lower magnification than the micrographs of nanocomposite just because of the different, i.e., higher, dimension of clay particles as received and after the compounding.

In more detail, 15A particles, i.e., tactoids of clay intercalated by the polymer chains, appears well distributed in all the cases, Figure 4(b–d), although when 10% of organoclay is used, Figure 4(d), it is possible to identify particles with larger dimensions, likely due to reaggregation phenomena caused by the too high concentration or, conversely, by a more difficult fragmentation.[26]

When 30B is used, the best morphology, particles dimension and distribution is obtained in the composites containing 3% of filler, Figure 4(f). In this case, the particles are even smaller and better distributed than the 15A ones even if voids are clearly visible on the fracture surface.

On increasing 30B concentration, the particles dispersion appears progressively worse and the dimension increased. Moreover a larger number of voids is visible. This latter phenomenon can be explained considering the above commented lower thermal stability of 30B. The product of degradation may reduce the affinity between the clay and the matrix, thus reducing the interfacial adhesion. The effect is more visible at higher clay content i.e., when higher is the amount of organic modifier available for degradation.

Melt rheology and intrinsic viscosity

In Figure 5 there are reported the viscosity curves as a function of frequency for neat PET and for all the nanocomposites. PET shows an almost Newtonian

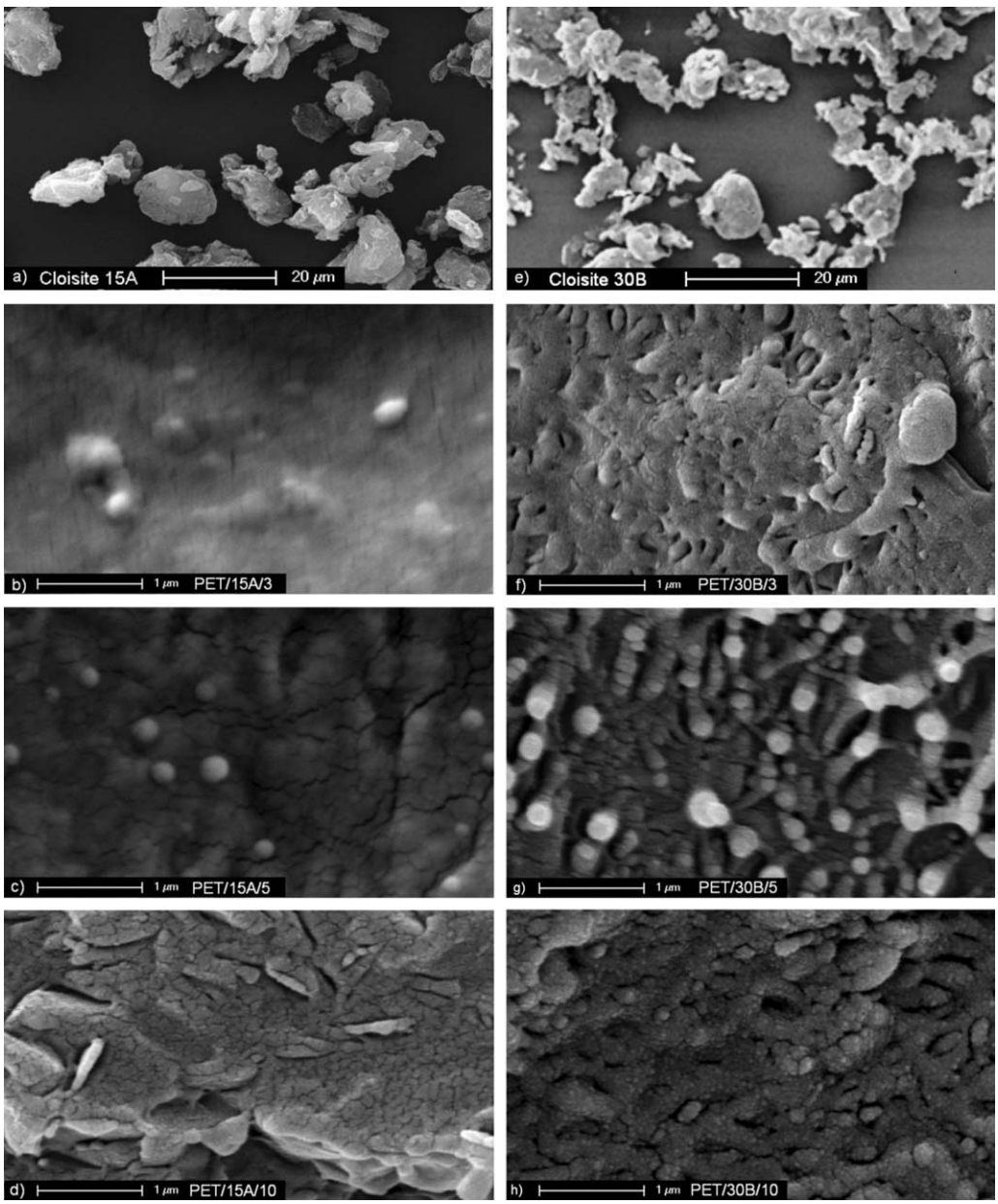

Figure 4 SEM micrographs of nanocomposite materials: (a) PET/15A/3; (b) PET/15A/5; (c) PET/15A/10; (d) PET/30B/3; (e) PET/30B/5; (f) PET/30B/10.

behavior in the whole frequency range here investigated. When 15A is added, the viscosity progressively increases on increasing the clay content even if some differences must be noticed. When 3% of 15A is added, the behavior remains almost Newtonian, but at 5 and 10% 15A content there is a sharp increase of the viscosity in the low frequency range, especially for the latter, indicating that the rheological behavior is dominated by the presence of the filler. At higher frequencies, the viscosity curve is almost coincident with that of the neat matrix, indicating that in this range, the rheological behavior is controlled by the matrix. These results are typical of nanostructured materials. In particular, it can be reasonably supposed that, above a certain critical amount, the filler is able to form a three-dimensional superstructure in which the tactoids interact each other.[30–32] Therefore, at low frequencies, i.e., at low stress level, the interactions prevail and the viscosity increases. On increasing the frequency i.e., the stress, the superstructure progressively disrupts and the viscosity become practically equal to that of the matrix.

The situation is different when 30B is added. The Newtonian behavior of the nanocomposite is observed for PET/30B/3 and PET/30B/5, but the viscosity is surprisingly lower than that of the neat matrix and lower when the filler content increases.

This decrease of viscosity can be explained considering—in full accordance with SEM and XRD

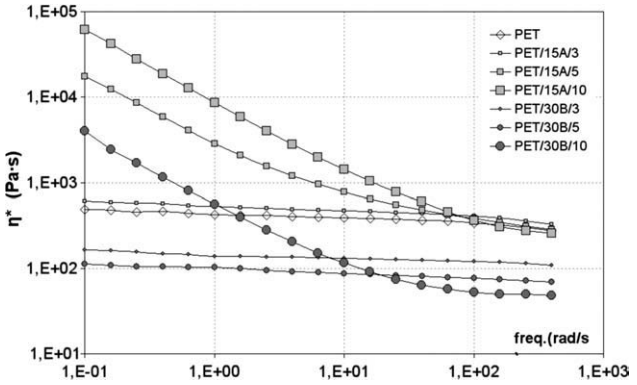

Figure 5 Flow curves of neat PET and of all PET based nanocomposites.

observation—relevant degradation phenomena of the matrix occurring during processing and involving the organic modifier of this specific organoclay sample. In particular, it can be hypothesized that the degradation products of 30B organic modifier accelerated the degradation of the PET matrix, thus causing a decrease of the melt viscosity. On increasing the 30B concentration, there is an increase of the total organic modifier amount that can undergo degradation and this can explain the decrease of viscosity in PET/30B5. Moreover, this interpretation is confirmed by the rheological curve of PET/30B/5. Similarly to what observed in 15A containing nanocomposites, at low frequencies it can be observed an increase of the melt viscosity due to the development of a three-dimensional network, as already commented above. At higher frequency, when the rheological behavior is dominated by the matrix, the viscosity drops to values lower than those observed when 5% was added.

To corroborate the hypothesis of a significant degradation of the matrix when interacting with the organic modifier of 30B, intrinsic viscosity measurements were carried out on all the materials prepared in the frame of this work.

To verify that the presence of the clay did not significantly influence the flow time and therefore the calculated intrinsic viscosity, we tested solutions containing clay amounts as high as those present in the nanocomposites. The results, indicated that the clay practically does not affect the flow time. Indeed the neat solvent and the solvent containing the clay shown respectively, a flow time of 60 s and 60.6 s.

In Table II there are reported the values of intrinsic viscosity obtained by using the Salomon-Ciuta formula (see experimental part). It is worth noting that, despite the measurement of the intrinsic viscosity by single-point determinations, can be affected by errors and the result may depend on the concentration, in our case (flexible polymer chains in good solvent) the values obtained can be considered exact.[33]

Virgin PET shows an intrinsic viscosity of 0.83 dL/g, in agreement with the value of the producer. The intrinsic viscosity is not significantly changing either after processing or after adding 15A. The situation is completely different when 30B is used instead. Adding only 3% of 30B causes a decrease of intrinsic viscosity from 0.83 dL/g to 0.72 dL/g and, on increasing the clay amount, the intrinsic viscosity progressively decreases to achieve 0.63 dL/g when 10% is added. This result confirms the hypotheses about the degradation of the PET matrix in the presence of 30B. Likely, the degradation products of the organic modifier induced and/or accelerated PET depolymerization causing a sharp decreasing of the molecular weight, thus confirming the results observed in the rheological behavior.

Thermal properties

Thermal properties of the nanocomposites were investigated by DSC measurements that were carried out on processed PET and on 3 and 10% nanocomposites. In Table III there are reported the calorimetric data for PET and for 3 and 10% containing nanocomposites after the first heating. The first heating, of course, gives information about the behavior of the materials as used for performing the mechanical testing. Considering the cold crystallization, PET is practically amorphous ($X_c \approx 0$). As a general comment, adding clay causes a decrease of the cold crystallization temperature and of the melting temperature together with an increase of cold crystallization enthalpy and melting enthalpy. The earlier cold crystallization can be explained considering the nucleating effect of the clays while the increase of crystallinity -even considering the neat value between melting and cold crystallization enthalpy- and the decrease of the melting temperature can be interpreted considering a reduction of the molecular weight.

Actually, some difference can be observed when using 15A or 30B. Adding 15A causes a only a slight and gradual decrease of the cold crystallization temperature and of the melting temperature together

TABLE II
Intrinsic Viscosity of All the Samples

Sample	Intrinsic viscosity (dL/g)
PET (virgin)	0.83
PET (extruded)	0.82
PET/15A/3	0.82
PET/15A/5	0.81
PET/15A/10	0.80
PET/30B/3	0.72
PET/30B/5	0.69
PET/30B/10	0.63

TABLE III
Calorimetric Data for PET and Selected Nanocomposites

Sample	ΔH_{cc} (J/g)	T_{cc} (°C)	ΔH_m (J/g)	T_m (°C)	ΔH_m-ΔH_{cc} (J/g)	X_c
PET (extruded)	24.18	126.5	−24.44	249.9	−0.26	0.2
PET/15/3	25.31	126.1	−26.16	249.6	−0.85	0.7
PET/15/10	26.09	124.8	−27.41	248.9	−1.32	1.1
PET/30B/3	26.16	118.3	−29.49	248.2	−3.33	2.8
PET/30B/10	26.14	116.7	−32.65	247.4	−6.51	5.5

with an increase of the melting enthalpy while these effects are definitely more intense when 30B is used. Again, to explain these results it can be hypothesized that a more pronounced degradation of PET matrix occurs when 30B is used. In particular, on decreasing the molecular weight, the chains become more mobile and more prone to form crystallites with, conversely, a reasonably lower regularity. This, together with the nucleating effect of the clay, implies a higher crystallinity but lower melting and cold crystallization temperatures.

Finally, the significantly higher crystallinity values observed for 30B containing materials are according with their slightly better mechanical performance if compared with the 15A containing ones.

Mechanical properties

In Table IV there are reported the Young's modulus, E, the tensile stress, TS and the elongation at break, EB, of all the materials prepared in the frame of this work.

For both series of materials, the modulus increases on increasing the amount of filler introduced and the highest values are achieved, for both filler used, when 10% is added.

This mechanical behavior is another indirect confirmation that the clay morphology achieved is intercalated and not exfoliated. The sharp increase of modulus, in fact, can be connected with the achievement of a percolation threshold that causes the formation of a 3D superstructure of clay platelets/tactoids.[30] In exfoliated nanocomposites this percolation threshold, in terms of weight percent of filler added, is reasonably very low and, however, well lower than 10%.[30] Of course, if only intercalated tactoids are present, the interactions among them and the consequent increase of resistance can generate only at high filler level, and this explains why significant increments of this property are observed only at 10% filler level. It is worth observing that there is practically no difference between the two fillers and this can be explained considering a balance between the particles dimensions and dispersion (better for 30B than for 15A) and the matrix degradation (stronger when 30B is used instead of 15A). Moreover, the higher cristallinity values observed for 30B containing materials due, as above commented, to the more intense degradation that occurs when 30B is used, are according with their slightly better mechanical rigidity if compared with the 15A containing ones.

As regards the elongation at break, it expectedly decreases on increasing the clay level for both 15A and 30B nanocomposites. The values observed for 30B nanocomposites are practically the same of 15A nanocomposites except for PET/30B/3. The better particles dimension and dispersion, as shown by TEM and SEM micrographs, can be invoked to explain this result. Indeed, the presence of large tactoids and clusters can act as a defect causing the premature breaking of the sample.

Tensile stress values follow the same trend shown by the elongation at the break. Indeed, 30B nanocomposites again show practically the same values of 15A nanocomposites except for the higher slightly value of PET/30B/3. This can be explained considering the higher elongation at break reached by this sample.

TABLE IV
Tensile Properties of All the Samples

Sample	E (MPa)	TS (MPa)	EB (%)
PET	987 ± 40	38.9 ± 2.6	80.7 ± 7.2
PET/15A/3	1015 ± 42	38.4 ± 2.4	4.9 ± 0.42
PET/15A/5	1086 ± 69	37.6 ± 3	4.6 ± 0.47
PET/15A/10	1730 ± 108	38.0 ± 3.1	2.7 ± 0.23
PET/30B/3	1063 ± 55	46.8 ± 1.9	13 ± 1.2
PET/30B/5	1149 ± 59	44.1 ± 2.1	5.1 ± 0.35
PET/30B/10	1831 ± 78	37.7 ± 4.1	2.4 ± 0.28

CONCLUSIONS

In this work we studied the properties of nanocomposites based on PET as matrix and two different samples of modified montmorillonites (15A, modified with a nonpolar organic salt and 30B, modified with a polar organic salt) prepared by melt extrusion. The results indicate that the most important factors affecting the performance of the nanocomposites are: the kind of clay modifier, its eventual degradation and the clay level.

30B containing nanocomposites show a slightly better morphology (dispersion, particle dimension) if compared with those containing 15A.

As regards the degradation of the organic modifier, it was demonstrated that at the processing temperature adopted, both clay modifiers degrade thus inducing/promoting the degradation of the PET matrix even if 30B provoke effects of a definitely higher magnitude.

A significant increase of the modulus is observed only at the highest clay level. Moreover, the mechanical performance of the nanocomposite is the result of a balance between the positive effect of introducing the OMMs and the negative effect of degradation phenomena induced by the presence of these fillers.

The authors thank Prof. P. Magagnini and Dr. S. Filippi (University of Pisa) for X-ray analyses.

References

1. Jancar, J.; Douglas, J. F.; Starr, F. W.; Kumar, S. K.; Cassagnau, P.; Lesser, A. J.; Sternstein, S. S.; Buehler, M. J. Polymer 2010, 51, 3321.
2. Choudalakis, G.; Gotsis, A. D. Eur Polym Mater 2009, 45, 967.
3. Paul, D. R.; Robeson, L. M. Polymer 2008, 49, 3187.
4. Utracki, L. A.; Sepehr, M.; Boccaleri, E. Polym Adv Technol 2007, 18, 1.
5. Tjong, S. C. Mater Sci Eng R 2006, 53, 73.
6. Ray, S.; Okamoto, M. Prog Polym Sci 2003, 28, 1539.
7. Xu, B.; Zheng, Q.; Song, Y.; Shangguan, Y. Polymer 2006, 47, 2904.
8. Scaffaro, R.; Botta, L.; Mantia, F. P. Macromol Mater Eng 2009, 294, 445.
9. Marras, S. I.; Zuburtikudis, I.; Panayiotou, C. J Mater Sci 2010, 45, 6474.
10. Gurmendi, U.; Eguiazabal, J. I.; Nazabal, J. Macromol Mater Eng 2007, 292, 169.
11. Wu, D. F.; Zhou, C. X.; Fan, X.; Mao, D. L.; Zhang, B. J Appl Polym Sci 2006, 99, 3257.
12. Giraldi, A. L. F.; Bizarria, M. T. M.; Silva, A. A.; Velasco, J. I.; d'Avila, M. A. J Appl Polym Sci 2008, 108, 2252.
13. Sanchez-Solís, A.; Romero-Ibarra, I.; Estrada, M. R.; Calderas, F.; Manero, O. Polym Eng Sci 2004, 44, 1094.
14. Calcagno, C. I. W.; Mariani, C. M.; Teiceira, S. R.; Mauler, R. S. Polymer 2007, 48, 966.
15. Frounchi, M.; Dourbash, A. Macromol Mater Eng 2009, 294, 68.
16. Xu, X.; Ding, Y.; Qian, Z.; Wang, F.; Wen, B.; Zhou, H.; Zhang, S.; Yang, M. Polym Deg Stab 2009, 94, 113.
17. Chang, J. H.; Mun, M. K. Polym Int 2007, 56, 57.
18. Lee, S. S.; Ma, Y. T.; Rhee, H. W.; Kim, J. Y. Polymer 2005, 46, 2201.
19. Tsai, T. Y.; Li, C. H.; Chang, C. H.; Cheng, W. H.; Hwang, C. L.; Wu, R. J. Adv Mater 2005, 17, 1769.
20. Chen, Z.; Luo, P.; Fu, Q. Polym Adv Technol 2009, 20, 916.
21. Eckel, D. F.; Balogh, M. P.; Fasulo, P. D.; Rodgers, W. R. J Appl Polym Sci 2004, 93, 1110, and references herein.
22. Botta, L.; Scaffaro, R.; La Mantia, F. P.; Dintcheva, N. T. J Polym Sci Part B: Polym Phys 2010, 48, 344.
23. Ou, C. F.; Ho, M. T.; Lin, J. R. J Polym Res 2003, 10, 127.
24. Fornes, T. D.; Yoon, P. J.; Paul, D. R. Polymer 2003, 44, 7545.
25. Cui, L.; Khramov, D. M.; Bielawski, C. W.; Hunter, D. L.; Yoon, P. J.; Paul, D. R. Polymer 2008, 49, 3751.
26. Ton-That, M.-T.; Perrin-Sarazin, F.; Cole, K. C.; Bureau, M. N.; Denault, J. Polym Eng Sci 2004, 44, 1212.
27. Shah, R. K.; Paul, D. R. Polymer 2006, 47, 4075.
28. Gilman, J. W.; Harris, R. H.; Shields, J. R., Jr.; Kashiwagi, T.; Morgan, A. B. Polym Adv Technol 2006, 17, 263.
29. Scaffaro, R.; Mistretta, M. C.; La Mantia, F. P. Polym Degrad Stab 2008, 93, 1267.
30. Wang, K.; Liang, S.; Deng, J.; Yang, H.; Zhang, Q.; Fu, Q.; Dong, X.; Wang, D.; Han, C. C. Polymer 2006, 47, 7131.
31. Prasad, R.; Pasanovic-Zujo, V.; Gupta, R. K.; Cser, F.; Bhattacharya, S. N. Polym Eng Sci 2004, 44, 1220.
32. Gupta, R. K.; Pasanovic-Zujo, V.; Bhattacharya, S. N. J Non--Newtonian Fluid Mech 2005, 128, 116.
33. Pamies, R.; Hernández Cifre, J. G.; del Carmen López Martínez, M.; Garcia de la Torre, J. Colloid Polym Sci 2008, 286, 1223.